International Conference on Mathematics, Computational Methods & Reactor Physics (M&C 2009)
Saratoga Springs, New York, May 3–7, 2009, on CD-ROM, American Nuclear Society, LaGrange Park, IL

FRAMEWORK FOR SIMULATION OF PELLET/CLADDING THERMAL INTERACTION (PCTI) FOR FUEL PERFORMANCE CALCULATIONS

G. Hansen, R. Martineau, C. Newman, and D. Gaston
Multiphysics Methods Group
Idaho National Laboratory
Idaho Falls, ID 83415-3840
http://www.inl.gov/multiphysics
Glen.Hansen@inl.gov

ABSTRACT

The accurate modeling of heat transfer across the gap between reactor fuel pellets and the protective cladding is essential to understanding fuel performance, cladding stress and behavior under extended burnup situations. The gap heat transfer impacts both the steady state power that a fuel can support and the transient temperature of the fuel during power excursions. Further, interaction between the heat transfer and pellet mechanics drive the geometry of pellet/cladding mechanical interaction, which influences the stress state in and thus the life of the cladding. This study presents a multidimensional approach for modeling the gap during a simulation where there can be significant motion between the pellet and cladding. A Jacobian-free Newton Krylov method is used to provide for fully-coupled solution of the coupled thermal contact and heat equations.

AMS subject classifications: 68U20, 65D30, 65M60, 74S05

Key words: reactor fuel performance, pellet cladding interaction, mortar method, dissimilar mesh interfaces

1. INTRODUCTION

In a light water nuclear reactor fuel, a column of fissile fuel pellets is enclosed by a protective metal cladding that serves to separate the pellets from the reactor coolant and to prevent the release of fission products into the coolant. One important design requirement for a reactor fuel is to develop a fuel configuration that preserves the integrity of the cladding during the lifetime of the fuel under operating conditions. The cladding integrity is affected by a host of issues including radiation induced creep and cladding stress. The stress state

within the cladding is strongly influenced by the forces applied to the cladding by the pellets, which is influenced by the thermal and radiation conditions the pellets have been subjected to during their lifetime. One very important effect governing the pellet temperature is the heat transfer between the pellet and the cladding. Figure 1 shows the relationship between the pellet and cladding, where the gap has been magnified for clarity.

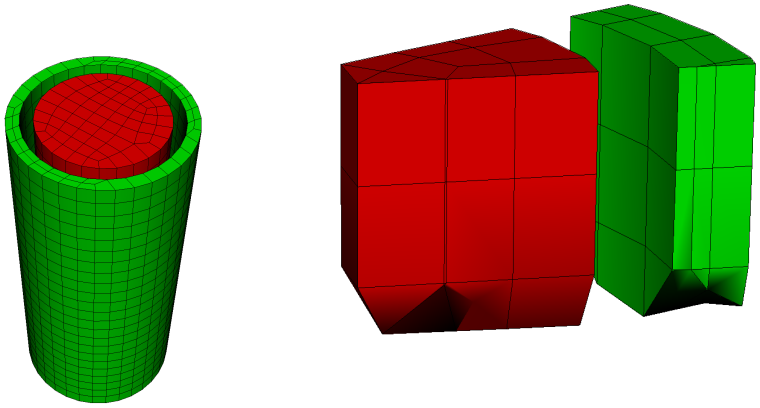

(a) Pellet and cladding **(b)** Closeup of the gap

Figure 1: Meshed representation of a fuel pellet surrounded by cladding. Right figure shows a closeup of the gap that separates the pellet and cladding (gap is exaggerated in this diagram).

The efficiency of heat transfer across the gap between the pellet and the cladding is a strong function of the instantaneous geometry of the pellet and cladding surfaces and any chemical action that has modified the surface properties over time. Further, this geometry is strongly three dimensional and stochastic, as it depends on the nature of thermally and fission product driven cracking of the pellet and relative motion between pellet fragments and the cladding.

Issues with modeling pellet / cladding interaction (PCI) have been recognized as a limitation with current fuel simulation codes. A recent report from the IAEA concluded that "Not many codes have good mechanical modeling capabilities, and the results that were obtained were limited" [1]. To begin to address this issue, this work proposes an implicit finite element method that supports the integration of the heat equation (1.1) across this gap for arbitrary meshed configurations of the pellet and cladding,

$$\rho(T)C_p(T)\frac{\partial T}{\partial t} - \nabla \cdot [k(T)\nabla T] = Q(T), \tag{1.1}$$

where T, ρ, C_p and k are temperature, density, specific heat, and thermal conductivity, and Q are internal heat sources. A finite element mortar method is used to model the gap, as

the relationship between the outside elements of the pellet mesh and the inside elements of the cladding mesh will change over time as the pellets expand axially with respect to the cladding.

The integration algorithm begins with the specification of bounding volumes that represent the region of influence for both cladding and pellet surface elements. A kD-tree spatial search [2] is performed to determine which bounding volumes potentially interact and thus participate in the transfer of heat from the pellet to the cladding. A modified mortar method is used to create a set of elements on which to integrate the heat equation and couple the thermal profile of the pellet to that of the cladding. As the pellet and cladding move relative to each other in a complex manner driven by instantaneous pellet temperature and fission product driven swelling, integration of the heat flow across the gap is a multiscale, multiphysics problem. As it is usually not necessary or desirable to resolve small scale transient behavior beyond initial thermomechanical equilibrium in a long-time pseudo-steady calculation, an efficient parallel implicit solution mechanism is required. As such, the proposed approach is based on a preconditioned Jacobian-free Newton Krylov (JFNK) solution method [3]. While this study is limited to a thermal analysis, it will ultimately be necessary to solve coupled thermal and mechanics equation systems [4] that govern heat flow in the fuel and the fuel's thermal and mechanical response.

2. MORTAR METHODS FOR PCTI

Figure 2 shows a hypothetical relationship between an element at the outside boundary of the fuel pellet that is transferring heat across the gap to an element of the cladding. For two and three-dimensional simulations, meshing and maintaining a mesh in the gap may not be tractable due to the relative motion between the pellet and cladding. The proposed method is based on developing a mortar element method [5–7] to form a finite element problem across the gap to support the solution of the heat equation. This approach is related to the method of Puso and Laursen [7]; in this case the pellet side of the interface will be the mortar side while the cladding surface is the non-mortar side. The proposed approach differs from mortar methods in the literature in the details of the discretization of the heat equation across the gap and by the use of the JFNK solution method to solve the coupled system.

The proposed algorithm begins with defining an surface-outward normal n to element face k. As k is generally non-planar, n is defined as the normal at the geometric center x_o of k. Further, p is the plane passing through x_o that n is normal to, as shown in Fig. 3.

Further, one may define a new polygon $\tilde{k}$ by projecting the corners of k onto p following n. A second polygon $\tilde{l}$ is formed by the projection of the corners of l onto p along n, shown in Fig. 4(a). The intersection of these facets $\tilde{k} \cap \tilde{l}$ is computed, resulting in the complex polygon shown in Fig. 4(b).

Lastly, Fig. 5 shows the use of the center of k to serve as a triangulation point of the polygon. Depending on the complexity of the polygon, a number n_p triangular pallets in p may be constructed.

This geometric description supports the development of a notation useful for defining a

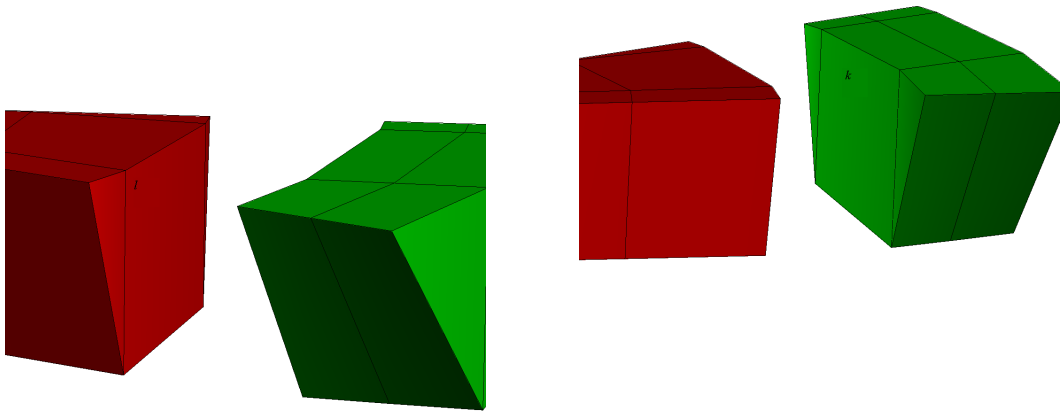

(a) Pellet view, element face l **(b)** Cladding view, element face k

Figure 2: Illustration of a scenario where an element at the boundary of the fuel pellet transfers heat across the gap to an element in the cladding. Element face l is the face of a pellet element exposed to the cladding, where element face k is the "closest" exposed cladding element face to l.

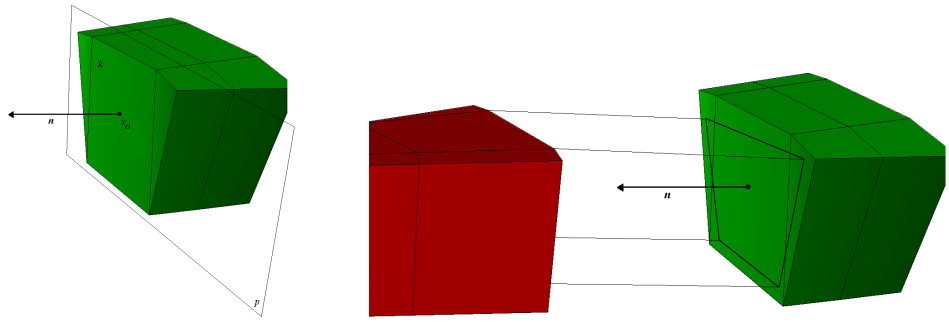

(a) Outward normal of plane p through x_o **(b)** Back-projection of nodes of l along n

Figure 3: The normal n to the plane p is normal to element face k at the geometric center x_o of k. Figure (b) shows a diagram denoting the projection of the corners of l onto plane p along the normal n.

common integration space between elements on the outside of the pellet and the inside of the cladding. This common space will host a finite element discretization of the heat equation, to support the calculation of heat transfer between the pellet and cladding. In the proposed method, a set of Gauss points are defined and positioned on each of the triangular pallets in p. These points are then projected along n onto the element faces k and l, which supports the definition of local parametric coordinates on these faces (with respect to p) of $\xi_{p,k}$ and $\xi_{p,l}$, respectively.

In the finite element method, it is customary to define element quantities $u(x, y, z)$ as a

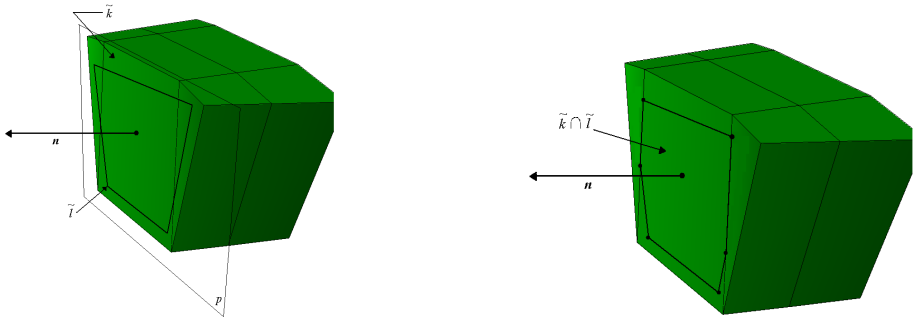

(a) New facets $\tilde{k}$ and $\tilde{l}$ on p **(b)** New polygonal facet $\tilde{k} \cap \tilde{l}$

Figure 4: A new complex polygon facet is formed by the intersection of $\tilde{k}$ and $\tilde{l}$.

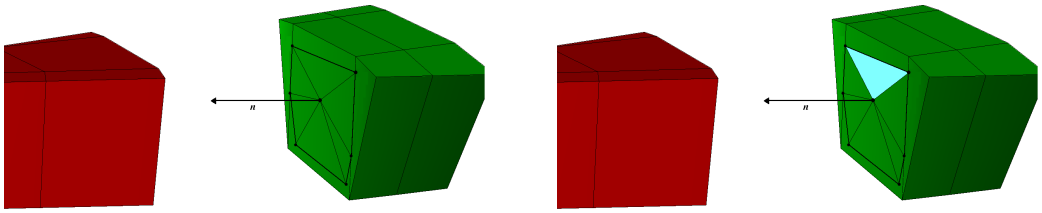

(a) Center x_o allows triangulation of the polygon **(b)** Triangular common integration face

Figure 5: Discretization of the polygon to form n_p triangular pallets.

series of test functions

$$u(x, y, z) = \sum_{j=1}^{N} u_j \Psi_j(x, y, z) = \sum_{j=1}^{N} u_j \psi(\xi),$$

where N is the number of Gauss points in the element and u is the element quantity of interest. With respect to the pallet p, one may define the integral contribution n^1_{AB} as

$$n^1_{AB} = A \sum_{j=1}^{N} \psi^1_A(\xi^1) \psi^1_B(\xi^1), \tag{2.1}$$

where the superscript 1 denotes that the expression is for the pellet surface, N is the number of Gauss points for the pallet being integrated, A is the area of that pallet, and the subscript A denotes the test function for the non-mortar side nodes is used (subscript B stands for the mortar side nodes).

To develop the composite heat equation and constraint problem across the gap, consider two subdomains, Ω_1 and Ω_2, with boundaries $\partial\Omega_1$ and $\partial\Omega_2$, exchanging heat along an interface defined by $\Gamma = \partial\Omega_1 \cap \partial\Omega_2$. The heat exchanging surfaces of each subdomain are defined by $\Gamma_1 = \Omega_1 \setminus \Gamma$ and $\Gamma_2 = \Omega_2 \setminus \Gamma$. The heat flux from Γ_1 and Γ_2 can be approximated by

$$q_1 = -k \frac{\partial T}{\partial n} \approx h(T_1 - T_2) \tag{2.2}$$

and

$$q_2 = k\frac{\partial T}{\partial n} \approx h(T_2 - T_1), \tag{2.3}$$

respectively. The normal vector n points inward from Γ_2 to Γ_1. The heat transfer coefficient h is defined as a combination of contact, radiation, and fluid resistances. T_1 and T_2 are the surface temperatures along Γ_1 and Γ_2. The physical constraint of this two body system is that the heat flux along Γ is continuous, or $q_1 = q_2$. The heat flux projected on Γ_1 from Γ_2 in terms of a Lagrange multiplier may be written as

$$\lambda = h(T_1 - T_2) \ , \tag{2.4}$$

which denotes the jump in temperature across Γ from subdomains Ω_1 and Ω_2.

Projecting the constraint in terms of the Lagrange multiplier onto both Ω and Γ will provide the coupling between the subdomains Ω_1 and Ω_2. In this context, equation (1.1) is recast as

$$\rho_I C_I \frac{\partial T_I}{\partial t} - \nabla \cdot k\nabla T_I + \lambda|_{\Gamma_I} = Q_I, \tag{2.5}$$

subjected to the constraint

$$h[T]_{\Gamma_I} - \lambda|_{\Gamma_I} = 0 \ , \tag{2.6}$$

where $[T]$ denotes the jump in temperature at the interface between the two subdomains. In equations (2.5) and (2.6), I refers to subdomain Ω_1 and Ω_2 or interface Γ_1 and Γ_2.

The mortar finite element method using dual basis functions for Lagrange multipliers [5] is based on the simultaneous solution of the weak form of equations (2.5) and (2.6). Defining Ω_1 as the mortar subdomain and Ω_2 as the non-mortar subdomain, the weak form of equations (2.5) and (2.6) may be recast in the matrix form as:

$$\begin{bmatrix} K_{11} & K_{12} & C \\ K_{21} & K_{22} & D \\ C^T & D^T & 0 \end{bmatrix} \begin{Bmatrix} T_1 \\ T_2 \\ \lambda \end{Bmatrix} = \begin{Bmatrix} Q_1 \\ Q_2 \\ 0 \end{Bmatrix} \tag{2.7}$$

3. SOLUTION FRAMEWORK

The code framework developed in this study is designed to support implementation of complex coupled multiphysics equation systems using a preconditioned Jacobian-free Newton Krylov architecture (JFNK; [3] and references contained therein). To summarize this approach in terms of the development of a fuel performance capability:

1. Finite element expressions for the thermomechanics, gap heat transfer, oxygen diffusion, mechanical contact, etc. form a nonlinear residual,

2. Newton's method is used to solve for a new problem state,

3. The Jacobian-free approximation is used to eliminate the need to form and store the Jacobian needed by Newton's method.

4. The Jacobian-free approximation also naturally supports effective coupling between physics and lends itself to an extensible and modular implementation in software.

Expression of the composite algebraic system in terms of a nonlinear residual function evaluation for use with the JFNK solution method begins with the indefinite system shown in (2.7), expanded as

$$\begin{bmatrix} K_{11} & K_{12} & 0 \\ K_{21} & K_{22} & 0 \\ 0 & 0 & 0 \end{bmatrix} \begin{Bmatrix} T_1 \\ T_2 \\ \lambda \end{Bmatrix} + \begin{bmatrix} 0 & 0 & C \\ 0 & 0 & 0 \\ C^T & 0 & 0 \end{bmatrix} \begin{Bmatrix} T_1 \\ T_2 \\ \lambda \end{Bmatrix} + \begin{bmatrix} 0 & 0 & 0 \\ 0 & 0 & D \\ 0 & D^T & 0 \end{bmatrix} \begin{Bmatrix} T_1 \\ T_2 \\ \lambda \end{Bmatrix} = \begin{Bmatrix} Q_1 \\ Q_2 \\ 0 \end{Bmatrix}. \tag{3.1}$$

This may be compactly written as three matvec additions,

$$\text{stiffness system} + \text{constraint system} + \text{dual basis system} - \text{sources} = 0. \tag{3.2}$$

This addition leads to the vector function

$$\mathbf{F}(\mathbf{x}) = \mathbf{0}\,, \tag{3.3}$$

that is of length N, where N is the number of unknowns in the discrete problem. The Jacobian of this system is a $N \times N$ sparse matrix,

$$\mathcal{J}(\mathbf{x}) = \frac{\partial \mathbf{F}(\mathbf{x})}{\partial \mathbf{x}}\,. \tag{3.4}$$

Given the Jacobian in this form, it is straightforward to express the Newton iteration,

$$\mathbf{x}^{(k+1)} \longleftarrow \mathbf{x}^{(k)} + \delta\mathbf{x}^{(k)}, \text{ and} \tag{3.5}$$

$$\mathcal{J}(\mathbf{x}^{(k)})\,\delta\mathbf{x}^{(k)} = -\,\mathbf{F}(\mathbf{x}^{(k)}), \tag{3.6}$$

where the superscript k denotes the iteration count of the Newton iteration. Using Newton's method as shown here amounts to implementing a sequence of steps:

1. Form the Jacobian matrix.

2. Solve the sparse linear system (3.6) to obtain $\delta\mathbf{x}^{(k)}$.

3. Apply this update (3.5) to obtain the next iteration of the solution state vector, $\mathbf{x}^{(k+1)}$.

Even for moderately-large grids, the cost of forming the Jacobian is high and typically dominates the computation, making the above algorithm impractical for most situations. Fortunately, Krylov iterative solvers such as the generalized minimum residual (GMRES) algorithm [9], which is used here to solve the Jacobian system, do not require the Jacobian matrix itself but simply the action of the Jacobian matrix on a vector. Approximating this matrix-vector product by differencing, which requires two nonlinear function evaluations, is

the basis of the JFNK method. Specifically, to evaluate the matrix-vector product $\mathcal{J}(\mathbf{x}^{(k)})\mathbf{v}$, a finite-difference approach,

$$\mathcal{J}(\mathbf{x}^{(k)})\mathbf{v} \approx \frac{\mathbf{F}(\mathbf{x}^{(k)} + \varepsilon\mathbf{v}) - \mathbf{F}(\mathbf{x}^{(k)})}{\varepsilon}, \tag{3.7}$$

is commonly used [3, 10]. Here, ε is chosen to avoid problems with machine precision.

Using this Jacobian-free approach, the dominant cost of the algorithm shifts from evaluating the Jacobian to the solution of the linear system. Indeed, the solution cost of GMRES for elliptic problems scales quadratically with the number of unknowns in the grid, unless effective preconditioning is used [11].

4. RESULTS

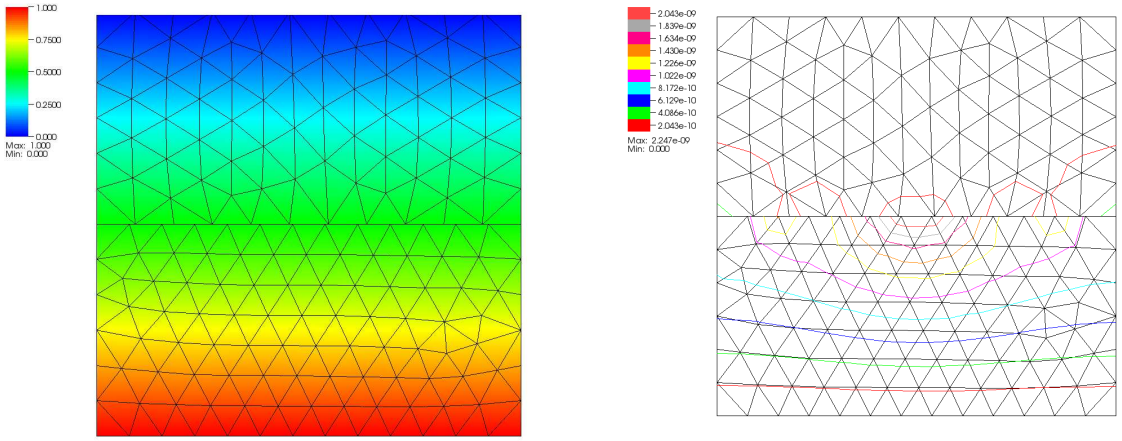

(a) Linear heat equation solution showing the horizontal nonconformal mesh contact interface

(b) Difference from exact solution, error $= u - u_h$

Figure 6: Solution of linear heat equation (1.1) (with constant coefficients); color denotes temperature. Left and right sides are insulated, $T = 0$ on top boundary and $T = 1$ on the bottom. Right figure shows that the maximum error is approximately 2×10^{-9} on this coarse mesh.

Figure 6 shows results on a simple validation problem that is based on a solution of the heat equation shown in (1.1) with constant coefficients $\rho C_p = 1$, $k = 1$, and $Q = 0$. Zero flux natural boundary conditions are imposed on the left and right boundaries. Essential boundary conditions of $T = 0$ and $T = 1$ are imposed on the top and bottom boundaries, respectively. The figure shows an unstructured triangle mesh on a two dimensional domain, but the problem as defined is one dimensional. Indeed, the exact solution is a linear profile vertically across the domain. Figure 6(b) shows error contours across the solution domain.

The contours indicate the magnitude of the error calculated from subtracting the computed solution from the exact solution error $= u - u_h$. The largest error obtained is approximately 2×10^{-9}. This error magnitude is quite good considering the coarse mesh employed. However, the solution is linear on this problem; this level of performance on nonlinear problems may be significantly more challenging to achieve.

Figure 7 shows a representative solution that involves a gap on a similar meshed domain. The gap is defined to correspond to the elements across the horizontal middle of the domain, directly below the nonconformal interface. Natural no flux conditions are again imposed on the left and right of the problem, and essential conditions of $T = 0$ and $T = 1$ are again imposed on the top and bottom of the domain. In this problem, a thermal conductivity of 1.0 is used for the material above the mortar interface and below the gap elements. The gap elements themselves employ a thermal conductivity of 0.111, calculated to preserve the conductivity ratio between uranium dioxide and helium at a temperature of 1000K, calculated using the correlations from Tables 1 and 2 of [4].

These results are two dimensional as the gap is not of uniform width across the center of the domain (it corresponds directly to the element height of the triangles shown in green in Fig. 7(a)). Further, note the significant temperature gradient in the gap shown by the contour lines, and in the profile along a vertical line in the center of the domain (see Fig. 7(b)).

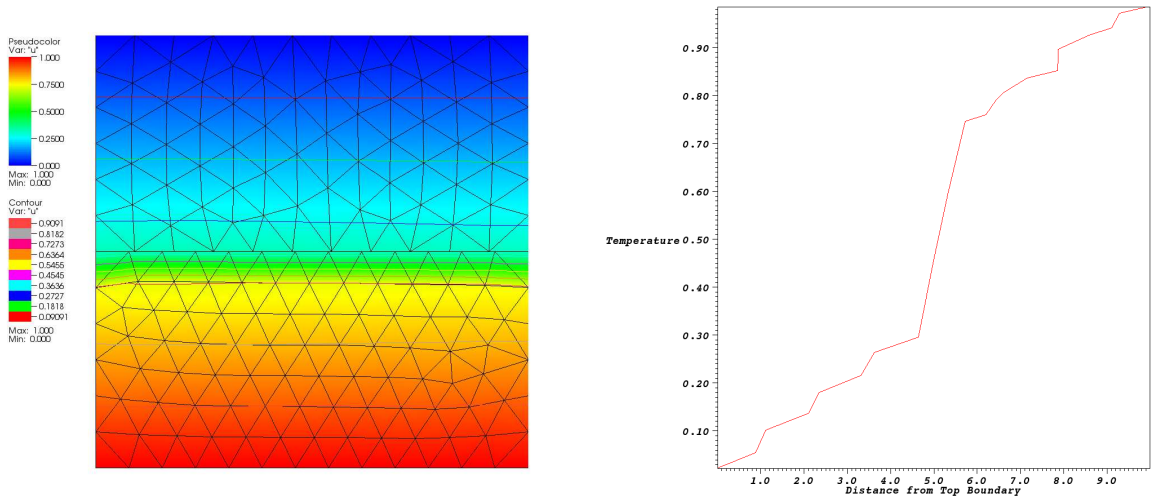

(a) Gap thermal solution

(b) Vertical temperature profile along a line midway from the left and right boundaries

Figure 7: Gap heat transfer solution using a thermal conductivity in the gap that is 10% of the conductivity in the upper and lower materials. The elements forming the gap are at the middle of the domain and are green in temperature. The mortar interface is directly above these elements; note that the mesh is nonconformal at this interface.

Future work begins with extending this implementation to three dimensions, verification of the spatial convergence of the method, and validation with a set of manufactured solutions.

Full pellet / cladding interaction capabilities will be achieved by adding the residual function evaluations, spatial searching, and mortar integration technologies developed here to the BISON fuel performance code described in [4].

ACKNOWLEDGMENTS

The submitted manuscript has been authored by a contractor of the U.S. Government under Contract No. DE-AC07-05ID14517 (INL/CON-08-15003). Accordingly, the U.S. Government retains a non-exclusive, royalty-free license to publish or reproduce the published form of this contribution, or allow others to do so, for U.S. Government purposes.

REFERENCES

[1] J. C. Killeen, J. A. Turnbull, and E. Sartori, "Fuel Modelling at Extended Burnup: IAEA Coordinated Research Project FUMEX-II," in "Proceedings of the 2007 International LWR Fuel Performance Meeting," San Francisco, California, Paper 1102 (September 30–October 3 2007).

[2] A. Khamayseh and G. Hansen, "Use of the Spatial kD-Tree in Computational Physics Applications," *Comm. Comput. Phys.*, **2**, 3, pp.545–576 (2007).

[3] D. A. Knoll and D. E. Keyes, "Jacobian-Free Newton-Krylov Methods: a Survey of Approaches and Applications," *J. Comput. Phys.*, **193**, 2, pp.357–397 (2004).

[4] C. Newman, G. Hansen, and D. Gaston, "Three Dimensional Coupled Simulation of Thermomechanics, Heat, and Oxygen Diffusion in UO_2 Nuclear Fuel Rods," *Journal of Nuclear Materials* (2009), in press.

[5] P. Wriggers, *Computational Contact Mechanics*, John Wiley and Sons Ltd., West Sussex, England, UK (2002).

[6] M. A. Puso and T. A. Laursen, "A Mortar Segment-to-Segment Contact Method for Large Deformation Solid Mechanics," *Comput. Methods Appl. Mech. Engrg.*, **193**, pp.601–629 (2004).

[7] M. A. Puso and T. A. Laursen, "A Mortar Segment-to-Segment Frictional Contact Method for Large Deformations," *Comput. Methods Appl. Mech. Engrg.*, **193**, pp.4891–4913 (2004).

[8] B. Wohlmuth, *Discretization Methods and Iterative Solvers Based on Domain Decomposition*, Lecture Notes on Computational Science and Engineering, Vol. 17, Springer Verlag, Heidelberg (2001).

[9] Y. Saad, *Iterative Methods for Sparse Linear Systems*, The PWS Series in Computer Science, PWS Publishing Company, Boston, MA (1995).

[10] M. Pernice and H. F. Walker, "NITSOL: a Newton iterative solver for nonlinear systems," *SIAM J. Sci. Comp.*, **19**, 1, pp.302–318 (1998).

[11] D. A. Knoll and W. J. Rider, "A Multigrid Preconditioned Newton-Krylov Method," *SIAM J. Sci. Comput.*, **21**, pp.691–710 (2000).